ACS APPLIED MATERIALS & INTERFACES

www.acsami.org

Research Article

Highly Stretchable and Conductive Self-Healing Hydrogels for Temperature and Strain Sensing and Chronic Wound Treatment

Jieyu Zhang, Can Wu, Yuanyuan Xu, Jiali Chen, Ning Ning, Zeyu Yang, Yi Guo, Xuefeng Hu,* and Yunbing Wang*

Cite This: *ACS Appl. Mater. Interfaces* 2020, 12, 40990–40999

Read Online

ACCESS | Metrics & More | Article Recommendations | Supporting Information

ABSTRACT: Flexible bioelectronics for biomedical applications requires a stretchable, conductive, self-healable, and biocompatible material that can be obtained by cost-effective chemicals and strategies. Herein, we synthesized polypyrrole or Zn-functionalized chitosan molecules, which are cross-linked with poly(vinyl alcohol) to form a hydrogel through dynamic di-diol complexations, hydrogen bonding, and zinc-based coordination bonds. These multiple dynamic interactions endow the material with excellent stretchability and autonomous self-healing ability. The choice of Food and Drug Administration (FDA)-approved materials (poly(vinyl alcohol) and chitosan) as the matrix materials ensures the good biocompatibility of the hydrogel. The conductivity contributed by the polypyrrole allowed the hydrogel to sense strain and temperature, and the coordinated Zn significantly enhanced the antibacterial activity of the hydrogel. Moreover, using a diabetic rat model, we have proved that this hydrogel is capable of promoting the healing of the infected chronic wounds with electrical stimulation.

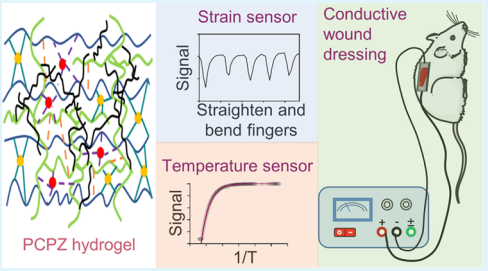

KEYWORDS: *conductive hydrogel, self-healing, flexible bioelectronics, biosensor, chronic wound*

1. INTRODUCTION

In recent years, the development of flexible wearable bioelectronics progresses rapidly. Nevertheless, a major obstruction to widespread applications is that most devices are unable to tolerate high strain and other mechanical impacts, and the durability needs to be further promoted. The rigid and brittle traditional electronic materials such as silicon and metals have low resistance to deformation. The electronic devices constructed with these stiff materials usually integrate poorly with soft organisms, resulting in a low signal/noise ratio and weak resistance to mechanical strain, which significantly prohibits their application in flexible bioelectronics. Various strategies have been developed to create flexible and stretchable circuits, including the development of flexible conductive polymers[1] or composites,[2] winding circuit interconnects (e.g., epidermal electronics),[3,4] and the integration of concentrated salts or ionic liquid into flexible gels[5] or microfluidic channels.[6] Although these techniques have led to different flexible bioelectronics, including wearable sensors,[7] flexible diagnostic devices,[3] and soft robots,[8] the products are typically susceptible to mechanical failure such as stretching, cutting, and twisting. When these devices are used on human skin or implanted in the human body, the multidimensional stress generated from daily human activities would damage the devices, and the repair is challenging or impossible. The damaging stress may be mitigated by the encapsulation of the soft circuits with rigid materials, but such packaging affects the flexibility and stretchability of the device.[9] Alternatively, a superior solution requires new materials that possess toughness, conductivity, and self-healing property.

Recently, efforts to develop self-healing conductive electronic materials have mainly focused on dynamic covalent bonds[10] and supramolecular systems based on singular noncovalent interactions such as hydrogen bonding,[11] crystallization,[12] ionic interaction,[13] and hydrophobic association.[14] Although these self-healing systems are promising for simple repairs, they suffer from at least one of the limitations, including a relatively long self-healing period; use of expensive, toxic, or hazardous materials; requirement for extrinsic stimuli such as solvent, thermal, light, or magnetic triggers; and relying on nonambient repair conditions.[9] Thus, overcoming these shortcomings is beneficial to improve the performance and durability of the flexible bioelectronics significantly.

Advanced materials with high stretchability and self-healing ability are essential for improving the durability of flexible bioelectronics. Even though some progress has been made in developing such materials,[9,13,15] the main limitations include sophisticated chemical reactions, expensive raw materials, and the possible harmful effect on the human body. In addition,

Received: May 6, 2020
Accepted: August 18, 2020
Published: August 18, 2020

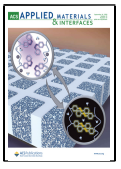

https://dx.doi.org/10.1021/acsami.0c08291
ACS Appl. Mater. Interfaces 2020, 12, 40990–40999

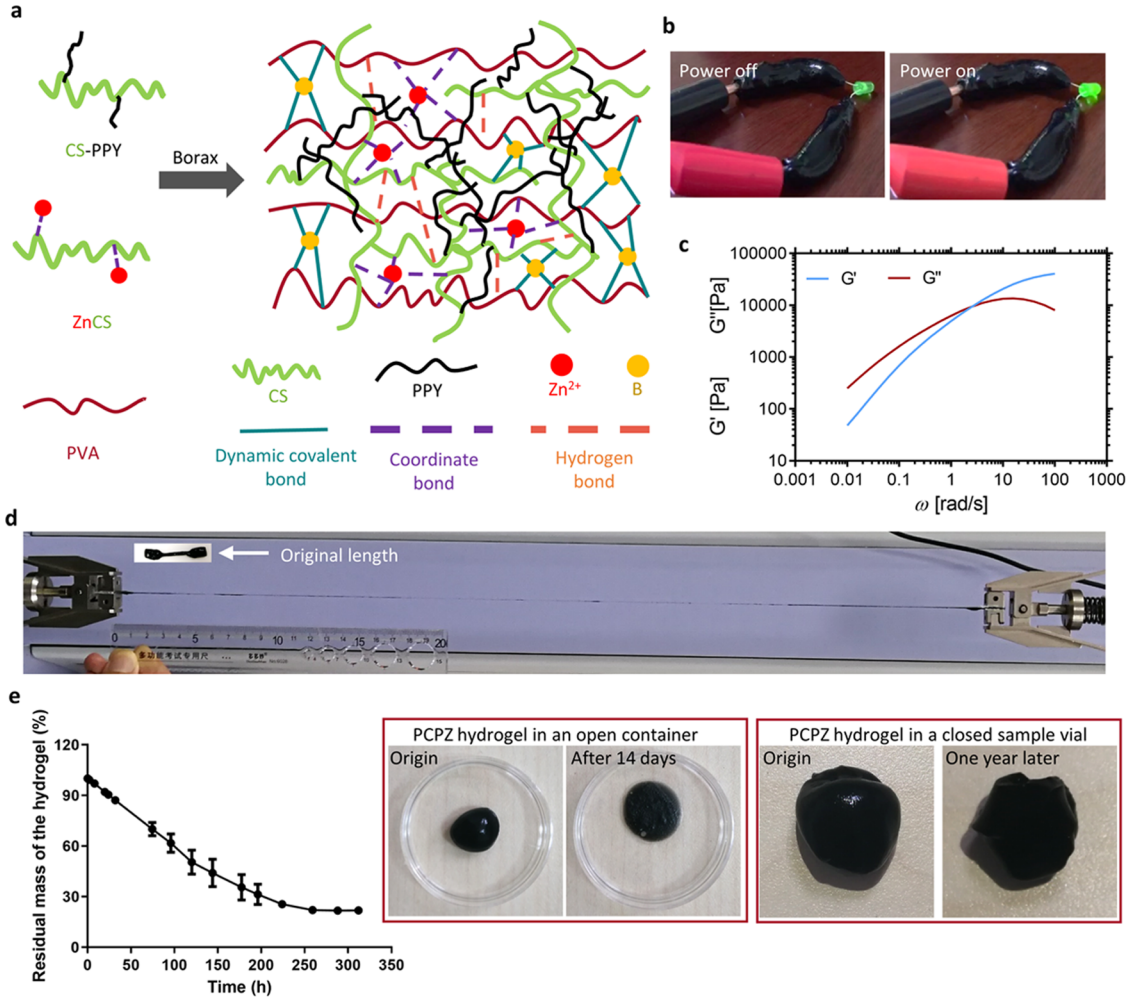

Figure 1. Designation and characteristics of the PCPZ hydrogel. (a) Schematic illustration of the preparation of the PCPZ hydrogel. (b) Circuit consisting of a light-emitting diode (LED) bulb and the PCPZ hydrogel, demonstrating that the hydrogel is conductive. (c) Rheological properties of the PCPZ hydrogel. (d) Photo of the PCPZ hydrogel after being stretched to the maximum stroke of the tensile testing apparatus. (e) Dehydration of the PCPZ hydrogel as indicated by the residual hydrogel mass when the hydrogel was in an open container under the ambient condition. The photos show the PCPZ hydrogel before and after dehydration in different containers, $n = 3$.

antibacterial performance has become increasingly important for flexible bioelectronics. The antibacterial properties help to reduce the frequency of replacement of the devices used in direct contact with the skin, which is home to bacteria, and prevent infections from the implanted devices. However, few investigations have focused on providing antibacterial properties for flexible bioelectronics. Herein, conventional and biocompatible polymers were used to create a flexible, conductive, and highly stretchable self-healing hydrogel with deformation- and temperature-sensitivity, which would be a promising candidate for fabricating flexible bioelectronics. First, polypyrrole (PPY) or Zn^{2+} was used to functionalize chitosan (CS) molecules to endow them with electrical conductivity or antibacterial properties, respectively. The reason behind choosing Zn^{2+} is because it is less toxic than other antibacterial ions such as Ag^{+}.[16] The functionalized CS and poly(vinyl alcohol) (PVA) were subsequently cross-linked by dynamic multiphysical and chemical interactions to form the hydrogel. These interactions can be easily broken and restored to dissipate energy on stretching and allow fast self-healing after damage. Besides, the conductivity can enable the hydrogel to sense temperature and strain based on the changes of resistance, and the antibacterial property is further favorable to biomedical applications.

2. RESULTS AND DISCUSSION

2.1. Material Design and Characterizations. As schematically illustrated in Figure 1a, the Food and Drug Administration (FDA)-approved materials, CS and PVA, were selected to build the framework of the hydrogel. The conductive component, PPY-grafted CS (CS-PPY), was synthesized by free-radical graft polymerization of PPY onto the double bond-decorated chitosan (DBCS). CS was also chelated with Zn^{2+} to prepare the antibacterial ZnCS (Figure S1a). A conductive, antibacterial, and highly stretchable hydrogel can be formed by merely mixing the CS-PPY, ZnCS, CS, PVA, and borax in one-pot via multiple cross-linking interactions. The PVA chains were covalently cross-linked by borax via the reversible di-diol complexation, and Zn^{2+} in the ZnCS cross-links the CS moieties via coordination bonds[17] (Figure S2). Another cross-linking interaction is the hydrogen bonding formed between −OH and $-NH_2$ groups of the different moieties in the hydrogel (Figure S2). Due to the dynamic characteristics of these cross-linking interactions, an

https://dx.doi.org/10.1021/acsami.0c08291
ACS Appl. Mater. Interfaces 2020, 12, 40990−40999

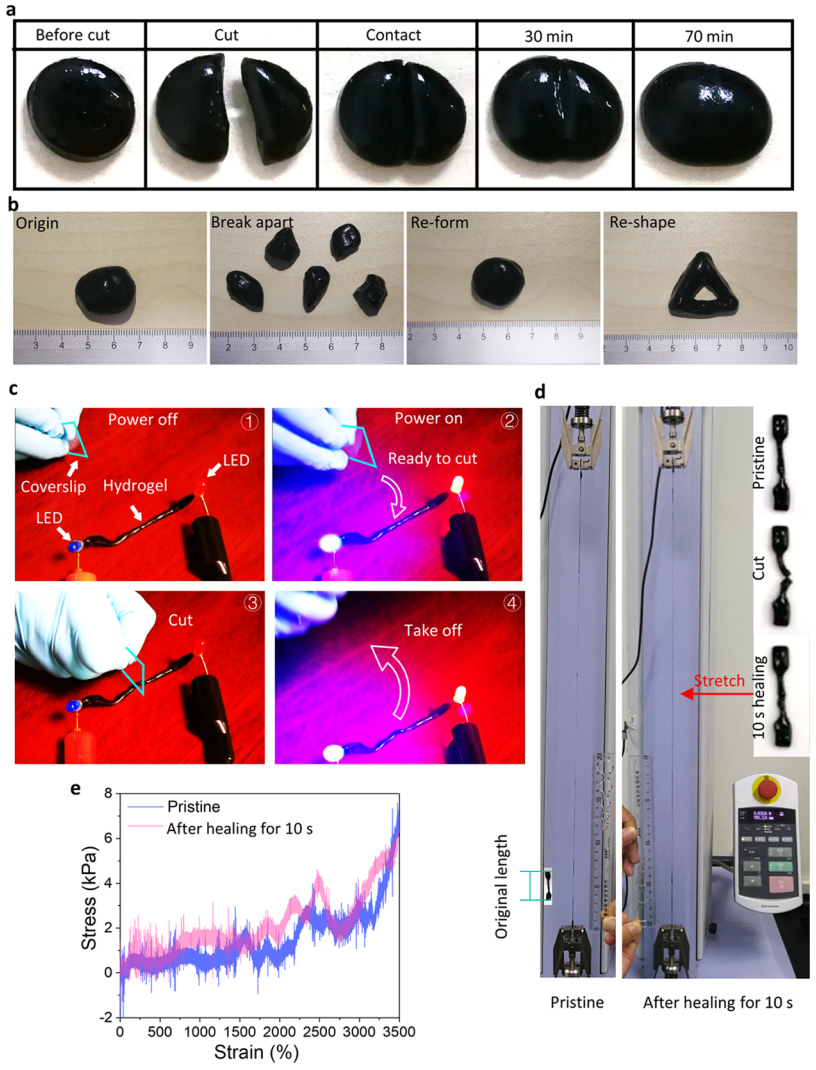

Figure 2. Self-healing behavior of the PCPZ hydrogel. (a) Photos showing the healing process in 70 min without applying any external stimuli. (b) Photos showing that the hydrogel can be broken apart, re-formed, and reshaped manually. (c) Photos showing the self-healable circuit constructed with the PCPZ hydrogel. (d) Photos of the healed PCPZ hydrogels that were stretched to the maximum stroke of the tensile testing apparatus. The insets show the photos of the PCPZ hydrogel in different states. (e) Tensile curves of the pristine and healed PCPZ hydrogels, as illustrated in (d).

intrinsically stretchable and self-healing conductor can be expected.

To optimize the properties of the hydrogel, the ratio of the components mentioned above was evaluated. First, minimum inhibition concentration (MIC) and minimum bactericidal concentration (MBC) were used to investigate the effect of the Zn/CS ratio on the antibacterial properties of ZnCS. When the Zn/CS ratio increases from 0.25 to 1, more Zn is coordinated with CS, and the antibacterial ability increases as indicated by the reduced MIC and MBC values (Figure S3). Thus, ZnCS is synthesized at Zn/CS = 1. Next, the matrix hydrogels were prepared with different ratios of PVA, borax, and CS (Table S1). The PVA/B2/CS2 (PC) hydrogel exhibits the highest gelling strength (Figure S4). The conductive component, CS-PPY, was then incorporated in the matrix PC hydrogel. The PPY moieties weaken the hydrogen bonding formed around CS and decrease the gelling strength of the prepared hydrogel (Figure S5). When the mass ratio of CS-PPY to the PVA solution exceeds 1% (the PVA/B2/CS2/CS-PPY1 (PCP) hydrogel), the conductivity of the hydrogel does not significantly increase with increasing CS-PPY content (Figure S6). The addition of 1% CS-PPY reaches the electrical percolation threshold to form long-range connectivity of conductive PPY segments in the hydrogel, and a further increase in the CS-PPY content does not significantly increase the conductivity. Finally, the antibacterial component, ZnCS, was added to the PCP hydrogel. With the mass ratio of ZnCS to the PVA solution ranging in 0.25−2%, the conductivity of the hydrogel does not change evidently while the gelling strength increases (Figures S5 and S6). Further increasing the amount of ZnCS results in phase separation, and in this situation, a homogeneous material cannot be obtained. Thus, to provide a substantial antibacterial property, the PCP hydrogel was supplemented with 2% ZnCS (the PCPZ hydrogel) for the following experiments.

The PCPZ hydrogel is electrically conductive (1.16 S/cm), which is illustrated by a circuit composed of a light-emitting diode (LED) bulb (Figure 1b, Movie S1). To examine the mechanical properties of the hydrogel, we carried out the rheological and tensile tests. Figure 1c shows that the storage modulus (G') of the PCPZ hydrogel is lower than the loss modulus (G'') at a low angular velocity, but with increasing

https://dx.doi.org/10.1021/acsami.0c08291
ACS Appl. Mater. Interfaces 2020, 12, 40990−40999

angular velocity, G' increases faster than G'', and the gel transition (when $G' = G''$) occurs at the angular velocity of 2.5 rad/s. This result suggests that with the angular velocity of ≥2.5 rad/s, the PCPZ hydrogel is a typically cross-linked polymer network. Nevertheless, before the gel transition, it can be expected that the fluid-like[15] material is highly stretchable. To further illustrate this aspect, we stretched the PCPZ hydrogel using a tensile test apparatus, and the material can be stretched to more than 35 times its original length without breaking (Figure 1d, at this point, the maximum stroke of the tensile test machine is reached). The high stretchability indicates that the PCPZ hydrogel has an efficient energy-dissipating ability.[18] In the PCPZ hydrogel, the di-diol complexation, Zn-based chelating, and hydrogen bonding form the dynamic inter and intrachain interactions (Figure S2). The intrachain interactions lead to the folding of the polymer chains, and the interchain interactions result in the hydrogel network. Upon stretching, the energy applied to the hydrogel is dissipated in two ways: (1) the breakage of the intrachain interactions results in the unfolding of the polymer chains, and (2) the breakage of the interchain interactions leads to sliding of the polymer chains. Simultaneously, due to the dynamic nature of these interactions, the broken bonds can be rapidly re-formed, which prevents the rupture of the material during stretching. With this exceptional mechanical property, the conductive PCPZ hydrogel is superior to most conventional hydrogels (which are usually fragile) for bioelectronic applications.

Besides poor mechanical behavior, another problem of conventional hydrogels is rapid dehydration in the ambient environment (commonly in several hours[19−21]), comprising its practical applications. As shown in Figure 1e, when the PCPZ hydrogel was placed in an open container in the ambient environment (25 °C and 60% humidity, the temperature and humidity were continuously recorded in Figure S7), it took 260 h for the hydrogel to dry to a constant weight. When the PCPZ hydrogel was kept in a capped sample vial, the appearance of the hydrogel did not visibly change even after 1 year storage (Figure 1e). The water in a hydrogel exists in two states, free water and bound water (binding with the hydrogel through different interactions such as hydrogen bonding and polar interaction). The water-retention ability of a hydrogel depends on the portion of bonded water because it is much more difficult than free water to evaporate. Thus, the high water-retention ability of the PCPZ hydrogel results from plenty of hydrophilic moieties (such as $-NH_2$, $-OH$, and Zn^{2+}) that bond with water (Figure S2) via hydrogen bonding or coordination bonds. In the literature, other strategies have also been developed to reduce hydrogel dehydration, including the addition of a high concentration of salts in the hydrogel to increase the portion of bonded water[20] or encapsulation of the hydrogel with a water-proof layer.[19] Although these methods work, high concentrations of salt are harmful to the body, and the encapsulation of a hydrogel is difficult for bioelectronic applications.

2.2. Self-Healing Behavior. The dynamic interactions in the PCPZ hydrogel can also result in self-healing property. The PCPZ hydrogel was cut into two parts, and the two parts were subsequently brought into contact. After 70 min, the interface between the halves spontaneously disappeared without applying any external stimuli (Figure 2a). Due to the self-healing property, the broken fragments of the hydrogel can also be immediately re-formed into the original shape and then reshaped by hands (Figure 2b). Moreover, a self-healable circuit was constructed with the PCPZ hydrogel and an LED bulb. Cutting the hydrogel thoroughly with a coverslip breaks the circuit (the bulb lit out), and the removal of the coverslip immediately restores the circuit's function (the bulb is relighted, Figure 2c, Movie S2). To further assess the healing property, the PCPZ hydrogel was cut into two pieces and recontacted for 10 s. The healed hydrogel can also be stretched to the maximum stroke (elongation of 3500%) without fracture by the tensile testing apparatus. The stress−strain curve of the healed hydrogel is similar to that of the pristine PCPZ hydrogel (Figure 2e), indicating effective healing in such a short time. Dynamic physical bonds (such as hydrogen bonding, hydrophobic association, and host−guest interaction) benefit rapid healing. For example, due to hydrogen bonding, a graphene oxide-based thermoreversible elastomer could recover 60% of its mechanical property after 60 s of healing.[22] However, the self-healing hydrogels based on dynamic physical bonds usually suffer from poor mechanical performance. A tough and self-healable poly(dimethylsiloxane) elastomer based on dynamic chemical coordination interactions was reported, but the healing was relatively slow (20% recovery of the mechanical property after 4 h).[15] In our PCPZ hydrogel, both the chemical (the di-diol and Zn−CS complexations) and physical (hydrogen bonding) cross-linking interactions are involved. The balance of these two types of interactions contributes to the rapid self-healing and high stretchability.

For biomedical applications, autoclaving or cryogenic storage is usually required, and it remains challenging to maintain the self-healing property after these operations. Figure S8 shows that the PCPZ hydrogel can tolerate autoclaving at 121 °C, and the autoclaved PCPZ hydrogel exhibits the same self-healing behavior as the hydrogel that does not undergo autoclaving. On the other hand, after freezing at −32 °C in a Leica CM1860 Cryostat, the PCPZ hydrogel fragments can be restored to their original state in 10 s (Figure S8b). To the best of our knowledge, the PCPZ hydrogel is the first material that exhibits autonomous self-healing after autoclaving and freezing at such a low temperature.

2.3. Application in Temperature and Strain Sensors. After evaluating the basic properties, we attempted to use the PCPZ hydrogel to fabricate temperature and strain sensors. The conductivity of the of PCPZ hydrogel results from the PPY moiety of CS-PPY. Due to the semiconductor nature, the conductivity (σ) should be affected by temperature in a relationship of $\sigma \propto e^{-E_g/T}$, where E_g and T refer to the band gap energy and temperature, respectively. To construct a temperature sensor using the PCPZ hydrogel, the hydrogel was encapsulated in a glass tube, and the two ends were connected to a multimeter (Figure 3a). This prototype was placed in an ice−water mixture with the temperature increasing from 0 to 43.5 °C. By monitoring the resistance of the sensor, the relationship between the temperature and the relative resistance change (defined as $\frac{R-R_0}{R_0}$, where R and R_0 indicate the instant resistance and initial resistance, respectively) is found to be in good agreement with the theoretical prediction curve ($R^2 = 0.9978$, Figure 3b) in the temperature range of 0−43.5 °C, and may be used for sensing temperature in biomedical applications. When the environment temperature is higher than 43.5 °C, the resistance change begins to deviate from the theoretical predictions.

https://dx.doi.org/10.1021/acsami.0c08291
ACS Appl. Mater. Interfaces 2020, 12, 40990−40999

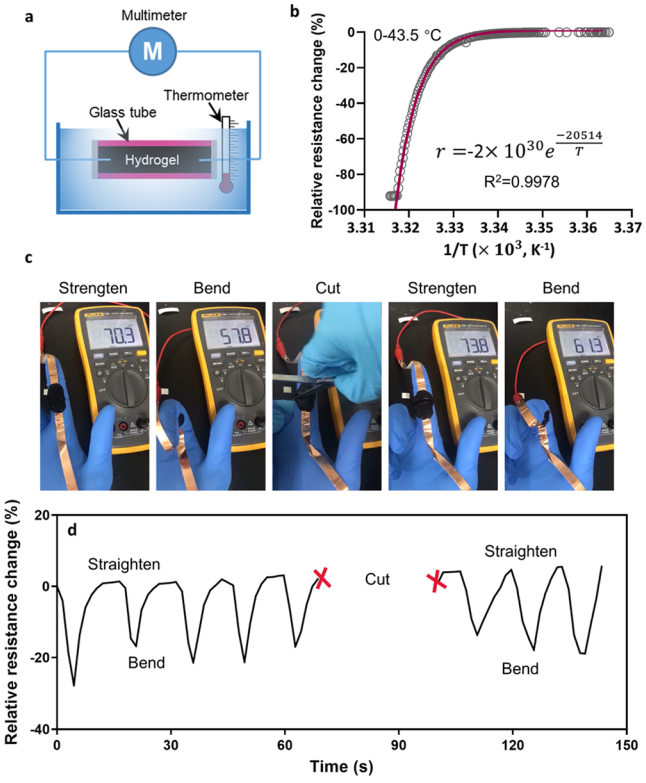

Figure 3. Illustration of the temperature and strain sensors established with the PCPZ hydrogel. (a) Schematic illustration of the temperature sensor fabricated with the PCPZ hydrogel. (b) Plot of relative resistance change vs temperature obtained with the temperature sensor. (c) Photos of the strain sensor constructed with the PCPZ hydrogel during finger movement monitoring before and after cutting with scissors. (d) Record of the relative resistance change of the PCPZ hydrogel when the finger is repeatedly bent and straightened before and after cutting with scissors.

From the definition of resistance $R = L/\sigma A$, where L and A represent the length and cross-sectional area of the specimen, it is known that R decreases when the specimen is compressed.[23] Hence, the flexible and conductive PCPZ hydrogel may also be applied for a strain sensor. To assemble a finger motion sensor, we attached the PCPZ hydrogel strip on the inside of an index finger with the two ends connected to a multimeter. Bending the finger results in the compression of the hydrogel, and thus reduces the resistance. While on straightening the forefinger, the resistance returns to its initial value. By monitoring the resistance signals, the bending and straightening of the finger can be recognized (Figure 3c), and the continuous record of the relative resistance change shows good reproducibility when the finger repeatedly bends and straightens (Figure 3d). Furthermore, due to its self-healing property, the sensor can still monitor the finger movement after cutting with scissors. Thus, the PCPZ hydrogel has good potential in monitoring body movement. Besides the movement monitoring, the electrical characterization of the hydrogel under static and cyclic strains was conducted, and the cyclic strain was generated using a mechanical testing machine. As shown in Figure S9, in a static state (strain = 0), the relative resistance change fluctuates around zero, whereas when the strain increases from 10 to 40%, the relative resistance change linearly (R^2 = 0.986) decreases from −11.9 to −37.5. This linear relationship between the relative resistance change and strain may endow the hydrogel with strain-sensing ability.

2.4. Application in Chronic Wound Treatment with Electrical Stimulation (ES). Besides sensors, the PCPZ hydrogel may also be applied as an advanced dressing in ES therapy for chronic wounds due to its conductivity and antibacterial ability. Chronic wounds that cannot simultaneously heal after 3 months[24] have become a serious global health problem, and traditional treatments such as debridement and negative pressure may not be effective.[25] As motivated by the fact that endogenous electric current arose at the wound site triggers the healing,[26] ES is becoming an auspicious therapy for chronic wounds due to its safety, inexpensiveness, facileness, as well as the improvement of the common deficiencies such as deficient cellular responses and insufficient blood flow.[27] In conventional ES treatment, separated electrodes are employed to apply an electric current, and this way of ES application is difficult to stimulate the whole wound bed that is deep, large, or irregularly shaped.[28] Overcoming this limitation requires the dressing capable of applying ES and completely covering the irregular wound bed. Thus, the PCPZ hydrogel would be a promising option owing to its flexibility and conductivity.

An ideal wound dressing should have good cytocompatibility, hemocompatibility, and antibacterial property. The leaching pattern test is a classical method for cytocompatibility assessment, and the result shows no cytotoxicity of the PCPZ hydrogel when fibroblasts are treated with the extract of the hydrogel or directly contact the hydrogel for 24 h (Figure 4a). The hemocompatibility of the PCPZ hydrogel was evaluated by the in vitro hemolysis assay using phosphate-buffered saline (PBS) and Triton X-100 as the negative and positive controls, respectively. The supernatant of the Triton X-100 group shows a bright red color due to significant hemolysis and release of hemoglobin. In contrast, similar to the PBS (a solution that does not induce hemolysis of erythrocytes) group, the supernatants of the PC, PCP, and PCPZ hydrogel groups are light yellow colored (Figure 4b). These results indicate the excellent hemocompatibility of the PCPZ hydrogel.

Antibacterial property is also essential for chronic wound treatment as ∼60% of chronic wounds suffer from infection.[29] Since chronic wound infection is regularly associated with bacterial biofilms,[30] the effect of the PCPZ hydrogel on biofilms was investigated. Figure 4c,d shows that treating *Staphylococcus aureus* or *Pseudomonas aeruginosa* (the most common pathogens in wound infection[31]) with the PC or PCP hydrogels cannot prevent the biofilm formation. However, when bacteria are treated with the PCPZ hydrogel, the bacterial density reduces by over six orders of magnitude as compared to the control (cultured without the hydrogel treatment). This result demonstrates that the PCPZ hydrogel can significantly inhibit biofilm formation, and the excellent antibacterial property originates from the ZnCS component. The antibacterial property of Zn^{2+} may result from the interfering effect on metabolism to form toxic secondary metabolites,[16] or inducing a Fenton reaction to produce reactive oxygen species (ROS) that can damage both the bacterial cell membrane and the proteins.[32]

To assess the space-filling property of the PCPZ hydrogel, we graved an irregular hole with sharp corners on a silicone plate to simulate a wound. Figure 5a shows that all of the corners are filled with the hydrogel, and the filled hydrogel can be entirely removed from the hole. This harsh simulation

https://dx.doi.org/10.1021/acsami.0c08291
ACS Appl. Mater. Interfaces 2020, 12, 40990−40999

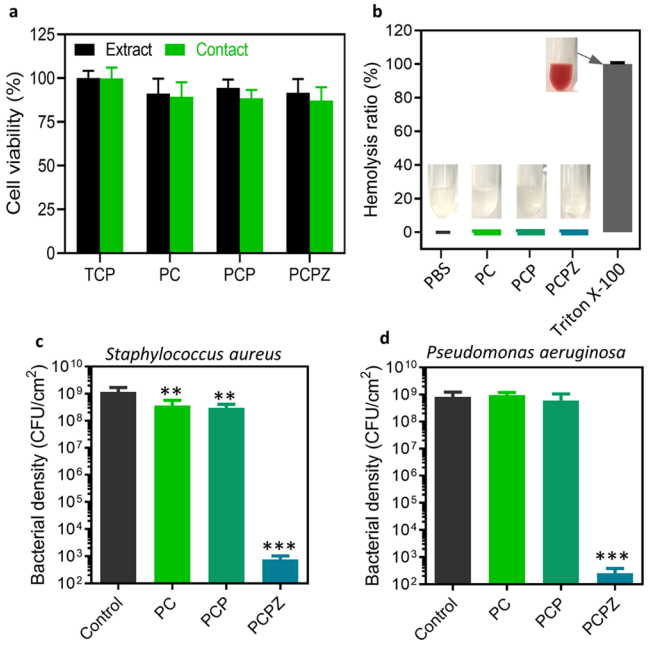

Figure 4. Biocompatibility and antibacterial property of the PCPZ hydrogel. (a) Cell viability of the different hydrogels assessed by the extract and direct contact method, $n = 3$. (b) Hemolysis ratio of the suspension of the different hydrogels. Triton X-100 that induces significant hemolysis was used as the positive control, and PBS, which does not hemolyze erythrocytes, was used as the negative control. The photos were obtained from the hemolysis assay, $n = 3$. (c). (d) Bacterial density of the biofilm on the agar gel beneath the different hydrogels after contacting for 24 h. The control indicates the bacterial density of the biofilm on the agar plate without any hydrogel treatment. * Indicates a significant difference compared with the control group, $n = 3$.

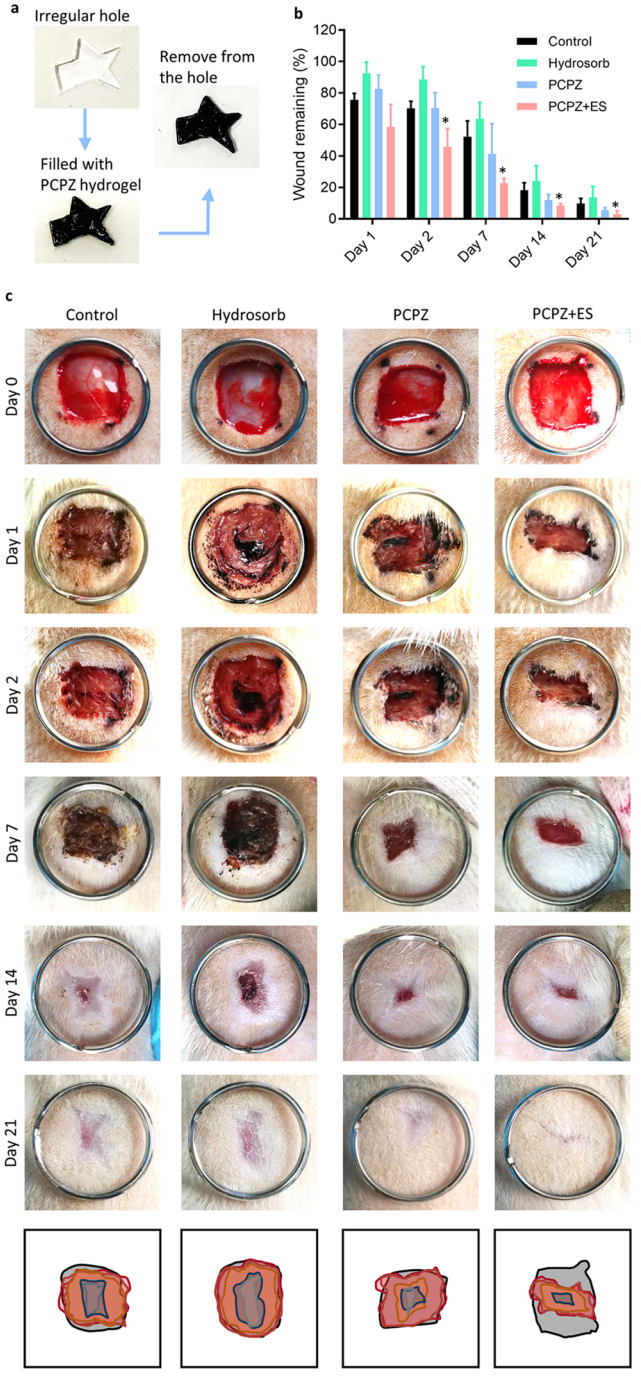

Figure 5. Application of ES through the PCPZ hydrogel for chronic wound treatment. (a) Photos showing the space-filling property of the PCPZ hydrogel. (b) Wound healing percentage of the different groups. * Indicates significant difference compared with the control group, $n = 3$. (c) Photos of the wounds of the different groups over 21 days. The bottom is the change of wound contour of the experimental groups over 21 days.

demonstrates that the PCPZ hydrogel can not only fill the irregular wound but also be easily removed when changing the dressing. Next, the PCPZ hydrogel was used as the conductive dressing to treat chronic wounds on a rat model with ES. Four groups of full-thickness wounds were created on each diabetic rat to generate chronic wounds. In the control group, the wound was not covered with a dressing, while in the Hydrosorb and PCPZ groups, the wound was treated with a commercial Hydrosorb dressing or a PCPZ hydrogel, respectively. For the PCPZ + ES group, the wound was treated with ES through a PCPZ hydrogel that covered the wound. All of the wounds were inoculated with *S. aureus* to induce infection. Figure 5b shows that the wounds are purulent on day 1, indicating that the wounds are infected. Compared with the control group, treating the wound with either the commercial Hydrosorb dressing or the PCPZ hydrogel alone does not accelerate the healing, but the stimulation of the wound with a voltage of 3 V though the conductive PCPZ hydrogel significantly promotes wound closure (Figure 5b,c). The histological results on day 21 (Figure 6) show that for the control group, a scab is still present on the wound with many blood cells in the dermis, suggesting that the wound is not completely closed yet. The healing extent of the Hydrosorb group is even worse than the control group, as indicated by the presence of the more massive scab on the wound. The Hydrosorb dressing contains a layer of the hydrogel (a hydrophilic polyurethane−polyurea hybrid), which releases moisture after application on the wound bed. Although the local humid environment can promote granulation, it does not work for infected wounds since the released moisture also benefits bacterial growth. For the PCPZ group, no scab is observed on the wound, and the injured epidermis and dermis heal. However, there are abundant blood cells in the dermis, indicating that the healing remains in the early proliferative phase. For the PCPZ + ES group, the collagen fibers in the dermis start to reorganize, and mature blood vessels are

https://dx.doi.org/10.1021/acsami.0c08291
ACS Appl. Mater. Interfaces 2020, 12, 40990−40999

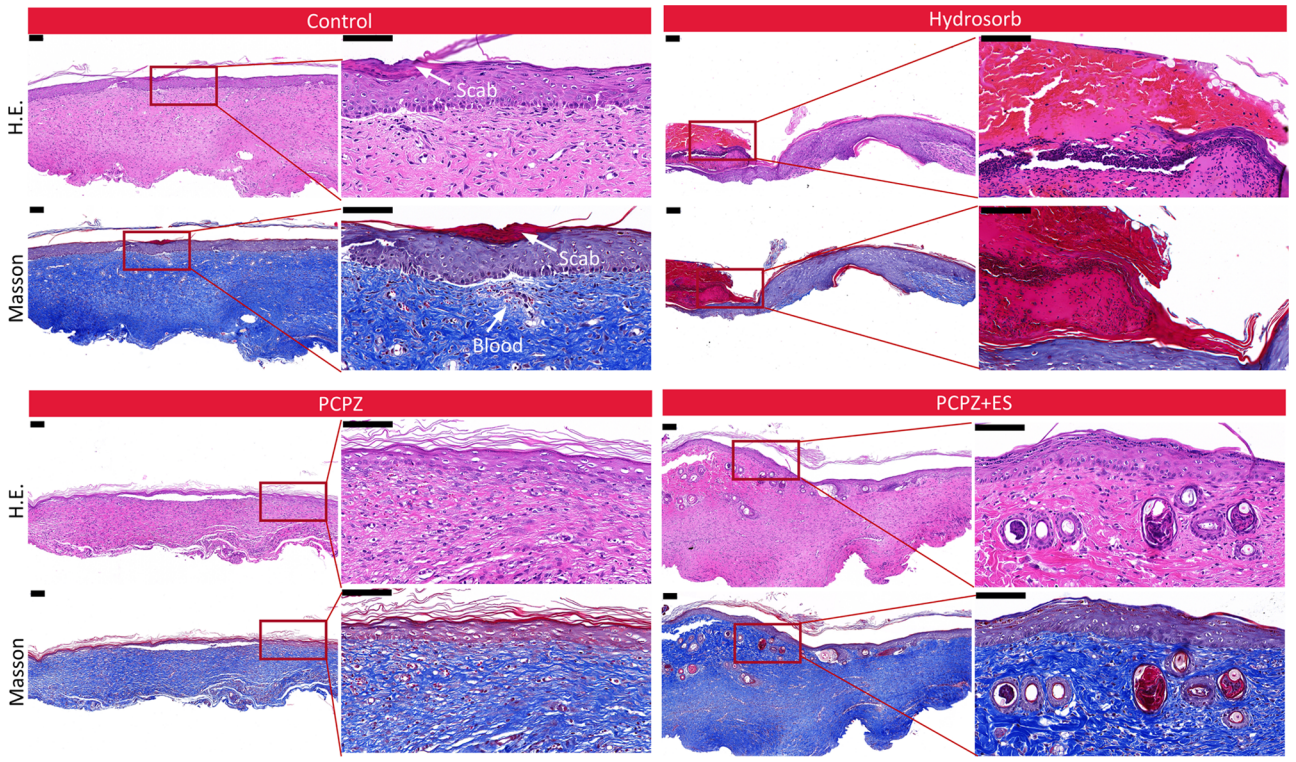

Figure 6. Hematoxylin & eosin and Masson staining of the sections of the regenerated tissues at the wound site on day 21 for the different groups. Scale bar = 100 μm.

observed. This result suggests that the application of ES through the PCPZ hydrogel is superior to using the hydrogel alone for the healing. The promoted healing of the infected wound in the PCPZ + ES group is probably due to the substantial antibacterial property of the PCPZ hydrogel (Figure 4c,d) and the promotion effect of ES on wound healing. The applied ES may maintain or enhance the cutaneous wound current, which triggers the healing.[33] ES may also promote the migration of fibroblasts and angiogenesis to accelerate wound closure, which is reported in our previous study[28] and the literature.[34]

3. CONCLUSIONS

A facile method is designed to prepare a highly stretchable conductive material with autonomous self-healing ability, which integrates several innovations. First, the PCPZ hydrogel is designed based on PVA and functionalized CS, which are cheap and easy to obtain. The facileness of the preparation strategy makes this biomaterial suitable for large-scale fabrication. Second, the combination of three multiple dynamic interactions (di-diol complexations, hydrogen bonding, and Zn-based coordination cross-linking) not only provides high stretchability but also results in excellent autonomous self-healing property. This aspect may inspire researchers to explore the combination of various dynamic bonds to address the challenges in material science using simple molecules. Third, the hydrogel is composed of biocompatible polymers, which allow direct contact with the human body, and its strong antibacterial ability is helpful for long-term utilization. With this material, the prototypes for different health-related applications are fabricated, and from the obtained results, we believe that the PCPZ hydrogel shows promise to construct flexible sensory systems and the next generation of smart biomedical products.

4. MATERIALS AND METHODS

4.1. Synthesis of ZnCS. ZnCS was prepared as per a reported procedure with modification.[35] CS (deacetylation degree ≥95%, Aladdin) was dissolved in 1% (v/v) acetic acid aqueous solution to prepare a 1% (w/v) CS solution. $ZnSO_4{\cdot}7H_2O$ (Alfa Aesar, 0.134, 0.268, 0.402, and 0.536 g, which corresponds to the Zn/CS ratios of 0.25, 0.5, 0.75, and 1, respectively) was added to 30 mL of the CS solution under stirring. After adjusting the pH value to 7.0 using 0.1 M ammonium hydroxide solution, the mixture was vigorously stirred for 3 h at 80 °C and then poured into 200 mL of acetone to precipitate ZnCS. The precipitated ZnCS was separated by filtration and washed twice with ethanol, followed by 48 h of freeze-drying.

4.2. Synthesis of CS-PPY. CS-PPY was synthesized according to earlier work with modification.[36] One gram of CS was dissolved in 50 mL of 2% (v/v) acetic acid aqueous solution, and 555 μL of methacrylic anhydride (Adamas-β) was added dropwise into the CS solution. The reaction was carried out under continuous stirring for 24 h at room temperature, and the product was dialyzed against deionized (DI) water for 3 days, followed by 48 h of freeze-drying to obtain the DBCS. Next, 578 μL of pyrrole was slowly added in a 0.1 M HCl solution containing 0.4% (w/v) DBCS followed by 2 h of stirring. Ammonium persulfate (APS, 0.38 g, Chron Chemicals) was added in the solution slowly with stirring. After 24 h of polymerization at room temperature, the mixture was poured into 300 mL of ethanol and kept at −20 °C for 30 min. The black precipitate (CS-PPY) was separated by centrifugation and washed twice with ethanol, followed by freeze-drying.

4.3. Preparation of the PCPZ Hydrogel. PVA (Chron Chemicals) was dissolved in DI water to form a 15% (w/v) PVA solution. Desired amounts of borax (Huaxia Reagent), CS, CS-PPY, and ZnCS were ground into fine powders with a mortar and then added in the PVA solution under mechanical stirring (Table S1). The mixture was homogenized by stirring for another 15 min to form the

https://dx.doi.org/10.1021/acsami.0c08291
ACS Appl. Mater. Interfaces 2020, 12, 40990−40999

hydrogels. The formula for preparing the hydrogels is listed in Table S1.

4.4. Characterization. Chemical structures of the compounds were characterized by nuclear magnetic resonance (NMR) and Fourier-transform infrared spectroscopy (FTIR). Rheological characteristics of the hydrogels were measured using a rheometer (MCR 302, Anton Paar), and the stress−strain analyses of the hydrogels were performed on a tensile test machine (EZ-LX, Shimadzu). The electrical conductivity of the hydrogel was measured using disk-shaped specimens (12 mm × 1 mm) on a digital four-point probe system (ST 2253, Jingge). The details are provided in the Supporting Information.

4.5. Cytotoxicity Assay. For the extract method, the hydrogels were cut into disk-shaped specimens (3.5 mm × 2 mm), and each sterile specimen was immersed in 3 mL of Dulbecco's modified Eagle medium (DMEM) for 24 h at 37 °C to prepare the hydrogel extract solution. For the direct contact method, the hydrogels were cut into disk-shaped specimens (8 mm × 2 mm), and the specimens were placed to contact cells cultured in a 24-well microplate. The details are provided in the Supporting Information.

4.6. Hemolytic Activity Assay. The hydrogels were freeze-dried and then dipped into liquid nitrogen for 5 min. After that, the frozen hydrogels were immediately grounded into a powder using a mortar and subsequently dispersed in PBS at the concentration of 5 mg/mL to prepare a hydrogel dispersion liquid. Sheep blood was centrifuged at 120*g* for 10 min at 4 °C, and the erythrocytes were diluted in PBS to obtain a 5% (v/v) erythrocyte suspension after three times of washing using PBS. Five hundred microliters of the erythrocyte suspension was mixed with 500 μL of the hydrogel dispersion liquid, PBS, or 0.1% Triton X-100, and the mixture was incubated at 37 °C for 1 h. After centrifuging at 120*g* for 10 min, 500 μL of the supernatants were transferred into a new tube and centrifuged at 12 000*g* for 10 min to remove the hydrogel particles. After that, 100 μL of the supernatants were transferred into a new 96-well plate, and OD_{540} was measured using a microplate reader. PBS and 0.1% (v/v) Triton X-100 served as the negative and positive controls, respectively. The hemolysis percentage of the hydrogels was calculated using the equation: hemolysis (%) = [(As − Ap)/(At − Ap)] × 100%, where As, Ap, and At represent the OD_{540} of the supernatants from the erythrocyte suspension treated with the hydrogel dispersion, PBS, and 0.1% Triton X-100, respectively.

4.7. MIC and MBC Measurement. The MIC and MBC of ZnCS for *S. aureus* (ATCC 25923) and *P. aeruginosa* (ATCC 27853) were tested by the broth microdilution method according to the recommendation of the Clinical Laboratory Standards Institute. The details are provided in the Supporting Information.

4.8. Effect of the Hydrogel on the Bacterial Biofilm Formation. The hydrogels were sterilized using an autoclave and punched into disk-shaped specimens (10 mm × 2 mm). One hundred microliters of bacterial suspension (1×10^7 CFU/mL) was spread on a growth agar plate, and the specimens were placed on the agar plate. After incubation at 37 °C for 24 h, the specimen and the agar beneath were collected for bacterial counting by the spread plate method.

4.9. Fabrication of the Temperature Sensor. The temperature sensor was prepared by filling the PCPZ hydrogel in a glass tube (diameter = 8 mm, length = 40 mm), and then connected to a digital multimeter (17B+, Fluke) at the two ends of the glass tube. The connections were sealed by a transparent tape, and the sensor was placed in an ice−water mixture (0 °C). When the temperature increased from 0 to 43.5 °C by slowly heating (1 °C/2 min), the resistance reading of the sensor was recorded by the multimeter.

4.10. Fabrication of Strain Sensor. The conductive PCPZ hydrogel (width = 15 mm, length = 30 mm, thickness = 1 mm) was attached on the inner side of the right index finger, and the two ends of the hydrogel were connected to a digital multimeter through double-sided copper tapes. The resistance was recorded on the bending and straightening of the index finger. To conduct the electrical characterization of the PCPZ hydrogel under static and cyclic strains, the hydrogel was shaped into a cuboid (10 mm × 10 mm × 15 mm) and mounted in a mechanical testing machine (UniVert, CellScale Biomaterials Testing). The two ends of the sample were connected to a multimeter for resistance measurement using double-sided copper tapes.

4.11. In Vivo Wound Healing Assay. All animal procedures were conducted according to the Guidelines for Care and Use of Laboratory Animals of Sichuan University. Streptozotocin was injected intravenously in the male Sprague Dawley (SD) rats (200−300 g) for type II diabetes mellitus induction at the dose of 60 mg/kg body weight until the fasting blood sugar level exceeded 16.67 mM.[37] The rats were anesthetized with 10% (w/v) chloral hydrate (0.3 mL/100 g body weight), and four full-thickness wounds (1 cm × 1 cm) were cut on the back of each rat. *S. aureus* suspension in PBS (10^8 CFU/mL) was injected at the wound to induce infection. The wounds were divided into four groups: In the control group, the wound was left untreated. For the Hydrosorb group, the wound was covered with a commercial Hydrosorb hydrogel. The wound covered with a PCPZ hydrogel was denoted as the PCPZ group. For the PCPZ + ES group, the wound was covered by a PCPZ hydrogel and stimulated by a direct current voltage of 3 V for 1 h per day. The ES treatment was carried out for 3 days, and the rats were euthanized after 21 days. The wound size was measured by tracing the wound boundaries on transparent plotting papers at predetermined time intervals. For the histopathologic examination, the regenerated skin was collected and fixed with neutral buffered formalin solution followed by embedment in paraffin. The sections (4 μm thickness) were stained with hematoxylin & eosin and Masson's trichrome reagents, respectively, and observed under a microscope (Eclipse TS2, Nikon).

4.12. Statistical Analysis. All data were obtained using the software, GraphPad Prism, version 8.0. The results are expressed as mean ± standard derivation ($n = 3$). A comparison between two groups was conducted using the two-tailed Student's *t*-test, and the comparison among more than two groups was carried out using one-way analysis of variance (ANOVA) with Tukey's post hoc test (*$p < 0.05$, **$p < 0.01$, and ***$p < 0.005$). Significance was accepted at $p < 0.05$, and the error bar in the figures indicates standard derivation.

■ ASSOCIATED CONTENT

Supporting Information

The Supporting Information is available free of charge at https://pubs.acs.org/doi/10.1021/acsami.0c08291.

Composition of different hydrogels (Table S1); schematic illustration of the hydrogel, FTIR and NMR of the key compounds, the rheological property, conductivity, environmental parameters for testing dehydration, self-healing ability, and strain-sensing ability of the hydrogels (Figures S1−S9) (PDF)

Conductivity of the PCPZ hydrogel (Movie S1) (MP4)

Rapid self-healing ability of the PCPZ hydrogel (Movie S2) (MP4)

■ AUTHOR INFORMATION

Corresponding Authors

Xuefeng Hu − *National Engineering Research Center for Biomaterials, Sichuan University, Chengdu, Sichuan 610065, China;* orcid.org/0000-0001-9683-3506; Email: huxuefeng@scu.edu.cn

Yunbing Wang − *National Engineering Research Center for Biomaterials, Sichuan University, Chengdu, Sichuan 610065, China;* orcid.org/0000-0002-2412-6762; Email: yunbing.wang@scu.edu.cn

Authors

Jieyu Zhang − *National Engineering Research Center for Biomaterials, Sichuan University, Chengdu, Sichuan 610065, China;* orcid.org/0000-0002-2827-3487

Can Wu − *National Engineering Research Center for Biomaterials, Sichuan University, Chengdu, Sichuan 610065, China*
Yuanyuan Xu − *National Engineering Research Center for Biomaterials, Sichuan University, Chengdu, Sichuan 610065, China*
Jiali Chen − *Department of Orthopaedics, West China Hospital of Sichuan University, Chengdu, Sichuan 610041, China*
Ning Ning − *Department of Orthopaedics, West China Hospital of Sichuan University, Chengdu, Sichuan 610041, China*
Zeyu Yang − *Rotex Co., Ltd, D6-1104, Chengdu, Sichuan 610064, China*
Yi Guo − *Rotex Co., Ltd, D6-1104, Chengdu, Sichuan 610064, China*

Complete contact information is available at: https://pubs.acs.org/10.1021/acsami.0c08291

Notes

The authors declare no competing financial interest.

■ ACKNOWLEDGMENTS

This work was supported by the National Natural Science Foundation of China (Grant no. 51803135), the China Postdoctoral Science Foundation (Grant no. 2018M640919), the Sichuan University Research Fund for Full-Time Postdoctoral (Grant no. 2018SCU12056), the Clinical Research Incubation Project (Grant no. 2019HXFH006), and the Special Fund for Nursing Discipline Development (Grant no. HXHL19003) of Discipline Excellence Development 135 Project of West China Hospital of Sichuan University. We would like to thank Prof. Liangyin Chu for the tensile test.

■ REFERENCES

(1) Bandodkar, A. J.; Lopez, C. S.; Mohan, A. M. V.; Yin, L.; Kumar, R.; Wang, J. All-Printed Magnetically Self-Healing Electrochemical Devices. *Sci. Adv.* **2016**, *2*, No. 1601465.
(2) Li, P. P.; Jin, Z. Y.; Peng, L. L.; Zhao, F.; Xiao, D.; Jin, Y.; Yu, G. H. Stretchable All-Gel-State Fiber-Shaped Supercapacitors Enabled by Macromolecularly Interconnected 3d Graphene/Nanostructured Conductive Polymer Hydrogels. *Adv. Mater.* **2018**, *30*, No. 1800124.
(3) Krishnan, S. R.; Ray, T. R.; Ayer, A. B.; Ma, Y. J.; Gutruf, P.; Lee, K.; Lee, J. Y.; Wei, C.; Feng, X.; Ng, B.; Abecassis, Z. A.; Murthy, N.; Stankiewicz, I.; Freudman, J.; Stillman, J.; Kim, N.; Young, G.; Goudeseune, C.; Ciraldo, J.; Tate, M.; Huang, Y. G.; Potts, M.; Rogers, J. A. Epidermal Electronics for Noninvasive, Wireless, Quantitative Assessment of Ventricular Shunt Function in Patients with Hydrocephalus. *Sci. Transl. Med.* **2018**, *10*, No. eaat8437.
(4) Kim, D.-H.; Lu, N.; Ma, R.; Kim, Y.-S.; Kim, R.-H.; Wang, S.; Wu, J.; Won, S. M.; Tao, H.; Islam, A.; Yu, K. J.; Kim, T.-i.; Chowdhury, R.; Ying, M.; Xu, L.; Li, M.; Chung, H.-J.; Keum, H.; McCormick, M.; Liu, P.; Zhang, Y.-W.; Omenetto, F. G.; Huang, Y.; Coleman, T.; Rogers, J. A. Epidermal Electronics. *Science* **2011**, *333*, 838−843.
(5) Kim, C.-C.; Lee, H.-H.; Oh, K. H.; Sun, J.-Y. Highly Stretchable, Transparent Ionic Touch Panel. *Science* **2016**, *353*, 682−687.
(6) Dickey, M. D. Stretchable and Soft Electronics Using Liquid Metals. *Adv. Mater.* **2017**, *29*, No. 1606425.
(7) Reeder, J. T.; Choi, J.; Xue, Y. G.; Gutruf, P.; Hanson, J.; Liu, M.; Ray, T.; Bandodkar, A. J.; Avila, R.; Xia, W.; Krishnan, S.; Xu, S.; Barnes, K.; Pahnke, M.; Ghaffari, R.; Huang, Y.; Rogers, J. A. Waterproof, Electronics-Enabled, Epidermal Microfluidic Devices for Sweat Collection, Biomarker Analysis, and Thermography in Aquatic Settings. *Sci. Adv.* **2019**, *5*, No. eaau6356.
(8) Li, T. F.; Li, G. R.; Liang, Y. M.; Cheng, T. Y.; Dai, J.; Yang, X. X.; Liu, B. Y.; Zeng, Z. D.; Huang, Z. L.; Luo, Y. W.; Xie, T.; Yang, W. Fast-Moving Soft Electronic Fish. *Sci. Adv.* **2017**, *3*, No. e1602045.
(9) Markvicka, E. J.; Bartlett, M. D.; Huang, X.; Majidi, C. An Autonomously Electrically Self-Healing Liquid Metal−Elastomer Composite for Robust Soft-Matter Robotics and Electronics. *Nat. Mater.* **2018**, *17*, 618−624.
(10) Wojtecki, R. J.; Meador, M. A.; Rowan, S. J. Using the Dynamic Bond to Access Macroscopically Responsive Structurally Dynamic Polymers. *Nat. Mater.* **2011**, *10*, 14−27.
(11) Xing, L.; Li, Q.; Zhang, G.; Zhang, X.; Liu, F.; Liu, L.; Huang, Y.; Wang, Q. Self-Healable Polymer Nanocomposites Capable of Simultaneously Recovering Multiple Functionalities. *Adv. Funct. Mater.* **2016**, *26*, 3524−3531.
(12) Nowak, A. P.; Breedveld, V.; Pakstis, L.; Ozbas, B.; Pine, D. J.; Pochan, D.; Deming, T. J. Rapidly Recovering Hydrogel Scaffolds from Self-Assembling Diblock Copolypeptide Amphiphiles. *Nature* **2002**, *417*, 424−428.
(13) Darabi, M. A.; Khosrozadeh, A.; Mbeleck, R.; Liu, Y. Q.; Chang, Q.; Jiang, J. Z.; Cai, J.; Wang, Q.; Luo, G. X.; Xing, M. Skin-Inspired Multifunctional Autonomic-Intrinsic Conductive Self-Healing Hydrogels with Pressure Sensitivity, Stretchability, and 3D Printability. *Adv. Mater.* **2017**, *29*, No. 1700533.
(14) Jeon, I.; Cui, J. X.; Illeperuma, W. R. K.; Aizenberg, J.; Vlassak, J. J. Extremely Stretchable and Fast Self-Healing Hydrogels. *Adv. Mater.* **2016**, *28*, 4678−4683.
(15) Li, C. H.; Wang, C.; Keplinger, C.; Zuo, J. L.; Jin, L.; Sun, Y.; Zheng, P.; Cao, Y.; Lissel, F.; Linder, C.; You, X. Z.; Bao, Z. A. A Highly Stretchable Autonomous Self-Healing Elastomer. *Nat. Chem.* **2016**, *8*, 619−625.
(16) Ning, C.; Wang, X. L.; Li, L. H.; Zhu, Y.; Li, M.; Yu, P.; Zhou, L.; Zhou, Z. N.; Chen, J. Q.; Tan, G. X.; Zhang, Y.; Wang, Y. J.; Mao, C. B. Concentration Ranges of Antibacterial Cations for Showing the Highest Antibacterial Efficacy but the Least Cytotoxicity against Mammalian Cells: Implications for a New Antibacterial Mechanism. *Chem. Res. Toxicol.* **2015**, *28*, 1815−1822.
(17) Zhang, H. C.; Jung, J.; Zhao, Y. Y. Preparation, Characterization and Evaluation of Antibacterial Activity of Catechins and Catechins-Zn Complex Loaded Beta-Chitosan Nanoparticles of Different Particle Sizes. *Carbohydr. Polym.* **2016**, *137*, 82−91.
(18) Zhao, X. Designing Toughness and Strength for Soft Materials. *Proc. Natl. Acad. Sci. U.S.A.* **2017**, *114*, 8138−8140.
(19) Yuk, H.; Zhang, T.; Parada, G. A.; Liu, X. Y.; Zhao, X. H. Skin-Inspired Hydrogel-Elastomer Hybrids with Robust Interfaces and Functional Microstructures. *Nat. Commun.* **2016**, *7*, No. 12028.
(20) Bai, Y. Y.; Chen, B. H.; Xiang, F.; Zhou, J. X.; Wang, H.; Suo, Z. G. Transparent Hydrogel with Enhanced Water Retention Capacity by Introducing Highly Hydratable Salt. *Appl. Phys. Lett.* **2014**, *105*, No. 151903.
(21) Yi, H.; Seong, M.; Sun, K.; Hwang, I.; Lee, K.; Cha, C.; Kim, T.-i.; Jeong, H. E. Wet-Responsive, Reconfigurable, and Biocompatible Hydrogel Adhesive Films for Transfer Printing of Nanomembranes. *Adv. Funct. Mater.* **2018**, *28*, No. 1706498.
(22) Wang, C.; Liu, N.; Allen, R.; Tok, J. B.-H.; Wu, Y.; Zhang, F.; Chen, Y.; Bao, Z. A Rapid and Efficient Self-Healing Thermo-Reversible Elastomer Crosslinked with Graphene Oxide. *Adv. Mater.* **2013**, *25*, 5785−5790.
(23) Lei, Z.; Wu, P. A Supramolecular Biomimetic Skin Combining a Wide Spectrum of Mechanical Properties and Multiple Sensory Capabilities. *Nat. Commun.* **2018**, *9*, No. 1134.
(24) Werdin, F.; Tenenhaus, M.; Rennekampff, H. O. Chronic Wound Care. *Lancet* **2008**, *372*, 1860−1862.
(25) Han, G.; Ceilley, R. Chronic Wound Healing: A Review of Current Management and Treatments. *Adv. Ther.* **2017**, *34*, 599−610.
(26) Zhao, M.; Song, B.; Pu, J.; Wada, T.; Reid, B.; Tai, G. P.; Wang, F.; Guo, A. H.; Walczysko, P.; Gu, Y.; Sasaki, T.; Suzuki, A.; Forrester, J. V.; Bourne, H. R.; Devreotes, P. N.; McCaig, C. D.; Penninger, J. M. Electrical Signals Control Wound Healing through Phosphatidylinositol-3-Oh Kinase-Gamma and Pten. *Nature* **2006**, *442*, 457−460.

(27) Sebastian, A.; Iqbal, S. A.; Colthurst, J.; Volk, S. W.; Bayat, A. Electrical Stimulation Enhances Epidermal Proliferation in Human Cutaneous Wounds by Modulating P53-Siva1 Interaction. *J. Invest. Dermatol.* **2015**, *135*, 1166−1174.
(28) Lu, Y.; Wang, Y.; Zhang, J.; Hu, X.; Yang, Z.; Guo, Y.; Wang, Y. In-Situ Doping of a Conductive Hydrogel with Low Protein Absorption and Bacterial Adhesion for Electrical Stimulation of Chronic Wounds. *Acta Biomater.* **2019**, *89*, 217−226.
(29) Cao, Y.; Tan, Y. J.; Li, S.; Lee, W. W.; Guo, H.; Cai, Y.; Wang, C.; Tee, B. C. K. Self-Healing Electronic Skins for Aquatic Environments. *Nat. Electron.* **2019**, *2*, 75−82.
(30) Buch, P. J.; Chai, Y.; Goluch, E. D. Treating Polymicrobial Infections in Chronic Diabetic Wounds. *Clin. Microbiol. Rev.* **2019**, *32*, No. e00091-18.
(31) Pfalzgraff, A.; Brandenburg, K.; Weindl, G. Antimicrobial Peptides and Their Therapeutic Potential for Bacterial Skin Infections and Wounds. *Front. Pharmacol.* **2018**, *9*, No. 281.
(32) Qin, H.; Zhao, Y. C.; An, Z. Q.; Cheng, M. Q.; Wang, Q.; Cheng, T.; Wang, Q. J.; Wang, J. X.; Jiang, Y.; Zhang, X. L.; Yuan, G. Y. Enhanced Antibacterial Properties, Biocompatibility, and Corrosion Resistance of Degradable Mg-Nd-Zn-Zr Alloy. *Biomaterials* **2015**, *53*, 211−220.
(33) Ashrafi, M.; Alonso-Rasgado, T.; Baguneid, M.; Bayat, A. The Efficacy of Electrical Stimulation in Lower Extremity Cutaneous Wound Healing: A Systematic Review. *Exp. Dermatol.* **2017**, *26*, 171−178.
(34) Funk, R. H. W. Endogenous Electric Fields as Guiding Cue for Cell Migration. *Front. Physiol.* **2015**, *6*, No. 143.
(35) Wang, X.; Du, Y. M.; Liu, H. Preparation, Characterization and Antimicrobial Activity of Chitosan - Zn Complex. *Carbohydr. Polym.* **2004**, *56*, 21−26.
(36) Darabi, M. A.; Khosrozadeh, A.; Mbeleck, R.; Liu, Y.; Chang, Q.; Jiang, J.; Cai, J.; Wang, Q.; Luo, G.; Xing, M. Skin-Inspired Multifunctional Autonomic-Intrinsic Conductive Self-Healing Hydrogels with Pressure Sensitivity, Stretchability, and 3d Printability. *Adv. Mater.* **2017**, *29*, No. 1700533.
(37) Dai, X.; Guo, Q.; Zhao, Y.; Zhang, P.; Zhang, T.; Zhang, X.; Li, C. Functional Silver Nanoparticle as a Benign Antimicrobial Agent That Eradicates Antibiotic-Resistant Bacteria and Promotes Wound Healing. *ACS Appl. Mater. Interfaces* **2016**, *8*, 25798−25807.

https://dx.doi.org/10.1021/acsami.0c08291
ACS Appl. Mater. Interfaces 2020, 12, 40990−40999